

Photovoltaic action of conjugated polymer/fullerene bulk heterojunction solar cells using novel PPE-PPV copolymers†

H. Hoppe,*^a D. A. M. Egbe,*^b D. Mühlbacher^c and N. S. Sariciftci^a

^aLinz Institute for Organic Solar Cells (LIOS), Johannes Kepler University, Altenbergerstr. 69, A-4040 Linz, Austria. E-mail: harald.hoppe@jku.at; Fax: (+43)-732-2468-8770; Tel: (+43)-732-2468-8854

^bInstitut für Organische Chemie und Makromolekulare Chemie, Friedrich-Schiller-Universität, Humboldtstr. 10, D-07743 Jena, Germany. E-mail: c5ayda@uni-jena.de; Fax: (+49)-3641-948202; Tel: (+49)-3641-948267

^cKonarka Austria, Altenbergerstr. 69, A-4040 Linz, Austria

Received 24th May 2004, Accepted 9th August 2004
First published as an Advance Article on the web 27th September 2004

The design of novel conjugated polymers suitable for use in plastic solar cells is one of today's challenges aiming towards improved key properties like the increase of photocurrent and open circuit voltage of such devices. In this work we present first results on arylene-ethynylene/arylene-vinylene hybrid polymers **3** (poly(-2,5-dioctyloxy-1,4-phenylene-diethynylene-2,5-dioctyloxy-1,4-phenylene-vinylene-2,5-di(2'-ethyl)hexyloxy-1,4-phenylene-vinylene)) and **5** (poly(2,5-dioctyloxy-1,4-phenylene-ethynylene-9,10-anthracenylene-ethynylene-2,5-dioctyloxy-1,4-phenylene-vinylene-2,5-di(2'-ethyl)hexyloxy-1,4-phenylene-vinylene)), demonstrating photovoltaic action in combination with the soluble C₆₀ derivative 1-(3-methoxycarbonyl) propyl-1-phenyl [6,6]C₆₁ (PCBM). Devices with an active layer thickness of about 100 nm yielded power conversion efficiencies of up to 2% under 100 mW cm⁻² AM 1.5 white light illumination. The coarse grained morphology of the active layers was identified as the main limitation for the photocurrent, revealed by AFM measurements. The photovoltaic devices were characterized by current–voltage and spectral photocurrent measurements. The results show that the open circuit voltage is weakly dependent on the HOMO (highest occupied molecular orbital) level of the conjugated polymer used as donor.

1. Introduction

Thin film organic (plastic) solar cells based on conjugated polymer/fullerene blends have become the subject of increasing interest within the past few years.^{1–3} As charge separation mechanism a fast photoinduced electron or hole transfer takes place between the electron donating and accepting species in the intermixed layer.⁴ The main characteristics of these bulk heterojunction devices is the highly increased interfacial area between the donor and acceptor phases as compared to bilayer heterojunctions, which enables charge separation throughout the film instead of just at a planar interface. Subsequently, the charges have to reach the opposite electrodes *via* percolating pathways in order to provide a photocurrent. The efficiency of poly-[2-(3,7-dimethyloctyloxy)-5-methyloxy]-*para*-phenylene-vinylene (MDMO-PPV) blended with [6,6]-phenyl C₆₁ butyric acid methyl ester (PCBM) based devices was increased recently from about 1% to 2.5% by changing the casting solvent.⁵ This increase can be understood by a change in the nanoscale morphology.^{6,7} For devices based on regioregular (poly(3-hexylthiophene-2,5-diyl) (P3HT) and PCBM, device efficiencies were raised to 3.5% as the photocurrent increased due to the lower band-gap of P3HT (~2.0 eV) as compared to MDMO-PPV (~2.2 eV).⁸ In order to reach commercially interesting conversion efficiencies of more than 5%, the photocurrent and the photovoltage have to increase further. As the photocurrent is ultimately limited by the optical band-gap of the polymer used, low-band-gap polymers are currently being introduced into plastic solar cells.^{9–11} Recently another approach to increase the absorption was to replace the C₆₀

derivative PCBM by a C₇₀ derivative, which exhibited an increased absorption in the longer wavelength range.¹² In the case of P3HT : PCBM blends the photocurrent was largely increased, but the open circuit voltage stayed far below that of MDMO-PPV based blends. Assuming reasonable ohmic contacts to anode and cathode, the open circuit voltage is ultimately limited in these devices by the difference between the electron affinity (LUMO level) of the acceptor (electron transporting species) and the ionization potential (HOMO level) of the donor (hole conducting species).^{13–15} Finally the resulting open circuit voltage can be influenced due to non-ohmic contacts with work functions lower or higher than the LUMO of the acceptor and the HOMO of the donor, respectively.^{16,17} Hence future improvement of the plastic solar cell depends on the synthesis of conjugated polymers with a lower band gap and larger ionization potential, to achieve higher photocurrents and voltages, respectively.

In this study we present first results on two hybrid arylene-ethynylene/arylene-vinylene^{18–21} polymers **3** and **5**, which potentially improve the open circuit voltage and the short circuit photocurrent at the same time. The increased open circuit voltage is a result of the electron-withdrawing nature of the –C≡C– moieties,²² leading to an enhanced electron affinity relative to MDMO-PPV, and consequently to a higher oxidation potential (improved oxidation stability) and a lower HOMO level (higher ionization potential). This has been confirmed by electrochemical methods in the present study. Moreover the presence of the electron rich anthracenylene units within the backbone of polymer **5** lowers the optical as well as the electrochemical band gap energies compared to MDMO-PPV. Spectral photocurrent measurements confirm that the absorption range is increased for blends of polymer **5** with PCBM as compared to MDMO-PPV.

† Electronic supplementary information (ESI) available: IR spectrum of polymer **5**. See <http://www.rsc.org/suppdata/jm/b4/b407794f>

2. Experimental

2.1 Materials

Poly(2,5-dioctyl-1,4-phenylene-diethynylene-2,5-octyloxy-1,4-phenylene-vinylene-2,5-di(2'-ethyl)hexyloxy-1,4-phenylene-vinylene) (3).

Polymer 3, whose synthesis has been described elsewhere, has the following characteristics: $\bar{M}_n = 24\,000\text{ g mol}^{-1}$, $\bar{M}_w = 70\,000\text{ g mol}^{-1}$, and polydispersity index = 2.9.²³

Poly(2,5-dioctyloxy-1,4-phenylene-ethynylene-9,10-anthracenylene-ethynylene-2,5-dioctyloxy-1,4-phenylene-vinylene-2,5-di(2'-ethyl)hexyloxy-1,4-phenylene-vinylene) (5).

9,10-Bis[(4-formyl-2,5-dioctyloxy)phenylethynyl]anthracene (4)²⁴ (1 g, 1.0555 mmol) and 2,5-di(2'-ethyl)hexyloxy-*p*-xylylene-bis(diethylphosphonate) (2)²⁵ (670 mg, 1.0555 mmol) were dissolved in dried toluene (40 mL) whilst stirring vigorously under argon and heating under reflux. Potassium *tert*-butoxide (480 mg, 4.28 mmol) was added to this solution, which rapidly became viscous. Another 10 ml toluene were added to the mixture; it was then heated at reflux for 3 h. After cooling to room temperature, 20 mL of 5% aqueous HCl solution were added. The organic phase was separated and extracted several times with distilled water until the water phase became neutral (pH = 6–7). The organic layer was dried in a Dean–Stark apparatus. The resulting toluene solution was filtered, evaporated under vacuum to *ca.* 10 ml and precipitated in methanol (200 ml). The polymer was extracted first with methanol (8 h), then with acetone (5 h). 1 g (77%) of dark red polymer was obtained. GPC (THF): $\bar{M}_w = 36\,000\text{ g mol}^{-1}$, $\bar{M}_n = 11\,000\text{ g mol}^{-1}$, $\bar{M}_z = 63\,000\text{ g mol}^{-1}$, polydispersity index = 3.0. ¹H NMR (250 MHz, CDCl₃): δ (ppm) = 0.78–2.09 (90H, bm, alkyl side chains), 3.41–4.06 (12H, bm, –CH₂O–), 6.80–6.87, 7.19, 7.53 and 8.79 (18H, arylene and vinylene H's). ¹³C NMR (62 MHz, CDCl₃): δ (ppm) = 11.44, 14.13, 22.69, 23.17, 24.05, 24.34, 26.19, 29.32, 29.46, 29.79, 30.68, 30.93, 31.87, 39.80 (alkyl side chains), 69.23, 69.73, 71.65 (–CH₂O–), 92.08 and 99.98 (–C=C–), 108.94, 109.96, 112.39, 117.01, 118.86, 122.73, 124.28, 126.53, 127.62, 129.28, 132.05, 150.39, 151.31, 154.58 (arylene and vinylene C's). IR (KBr): 3057 (w, C_{aryl}–H), 2954, 2923 and 2855 (vs, CH₃ and –CH₂–), 2185 (vw, –C=C–), 1598 (w, –C=C–_{aryl}), 1198 (s, C_{aryl}–OR), 966 (m, *trans* –CH=CH–) cm^{–1}. UV-Vis (CHCl₃, 9.0 × 10^{–6} M): λ_{max} /nm (ϵ /L mol^{–1} cm^{–1}) 265 (65 000), 320 (27 000), 540 (77 300). Anal. Calc. for (C₈₈H₁₂₀O₆)_{*n*}: C, 82.87; H, 9.49. Found: C, 81.73; H, 9.24%.

Poly[2-(3,7-dimethyloctyloxy)-5-methoxy-*p*-phenylene-vinylene] (MDMO-PPV) obtained from Covion (Germany) was also investigated for the purpose of comparison. Its chemical structure and that of PCBM ((1-(3-methoxycarbonyl)propyl-1-phenyl [6,6]C₆₀) are depicted in Fig. 1. PCBM was purchased from J. C. Hummelen (Univ. of Groningen, The Netherlands).

We used poly[3,4-(ethylenedioxy)thiophene] : poly(styrene sulfonate) (PEDOT : PSS, Baytron PH) from Bayer (Germany) as anode. As transparent conducting substrates we used ITO glass, purchased from Merck (Germany). The cathode

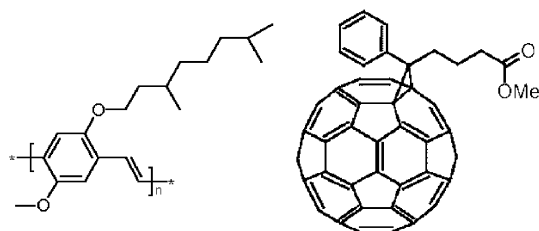


Fig. 1 Chemical structures of MDMO-PPV (left) and the soluble fullerene derivative PCBM (right).

materials used were evaporated aluminium in combination with a thin LiF interlayer.

2.2 Device preparation

After etching a part of the ITO glass to allow for selective contacting of the back electrode, films of PEDOT : PSS were spin cast at 1500 rpm from 0.5% aqueous solution onto the ITO substrate. Next, the photoactive layer was spin cast from chlorobenzene solution at 1500 rpm. The PCBM content of these solutions varied between 66% and 80%. Finally the top aluminium electrode was evaporated in a vacuum chamber. Cell areas varied between 10–20 mm². A schematic of the device structure is shown in Fig. 2.

2.3 Characterization methods

The methods and instrumentations for the chemical structure characterization of the polymers (¹H and ¹³C NMR, Infrared, UV-Vis, elemental analysis) as well as for the determination of the molecular weights and the investigation of the thermal behavior have been described elsewhere.^{24,25} Quantum-corrected emission spectra were measured in dilute chloroform solution with an LS 50 luminescence spectrometer (Perkin-Elmer). Photoluminescence quantum yields were calculated according to Demas and Crosby²⁶ against quinine sulfate in 0.1 N sulfuric acid as a standard ($\phi_{\text{fl}} = 55\%$). The solid films (cast from chlorobenzene solution) absorption and emission were measured with a Hitachi F-4500. The fluorescence quantum yield in the solid state was determined relative to a CF₃-PPV (poly{1,4-phenylene-[1-(4-trifluoromethylphenyl)-vinylene]-2,5-dimethoxy-1,4-phenylene-[2-(4-trifluoromethylphenyl)vinylene]}) copolymer reference whose fluorescence quantum yield has been measured by integrating sphere to be 43%.²⁴

The solar cell devices were characterized by current–voltage (*I*–*V*) measurements and by spectral photocurrent, *i.e.* incident photon to collected electron (IPCE), measurements under argon atmosphere. To determine the solar power conversion efficiency, *I*–*V* measurements under 80 mW cm^{–2} white light illumination from a Solar Constant 575 (K.H. Steuernagel, Germany) solar simulator were carried out. Spectral photocurrent was recorded under illumination of a monochromatized xenon lamp with a typical illumination density of 5–10 μ W. The incident beam was chopped with a mechanical chopper, the photocurrent was detected with a lock-in-amplifier. The Xe lamp spectrum was measured with a calibrated Si diode.

To characterize the HOMO–LUMO levels of the materials, cyclic voltammetry (CV) and electrochemical voltage spectroscopy (EVS) measurements were performed. Electrochemical measurements were carried out at room temperature in a glove-box using a Jaisle potentiostat computer controlled with SCADA software. The supporting electrolyte was 0.1 M (C₄H₉)₄N⁺PF₆[–] in acetonitrile, the working and counter

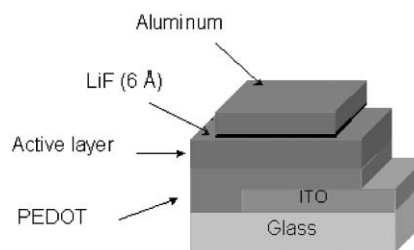
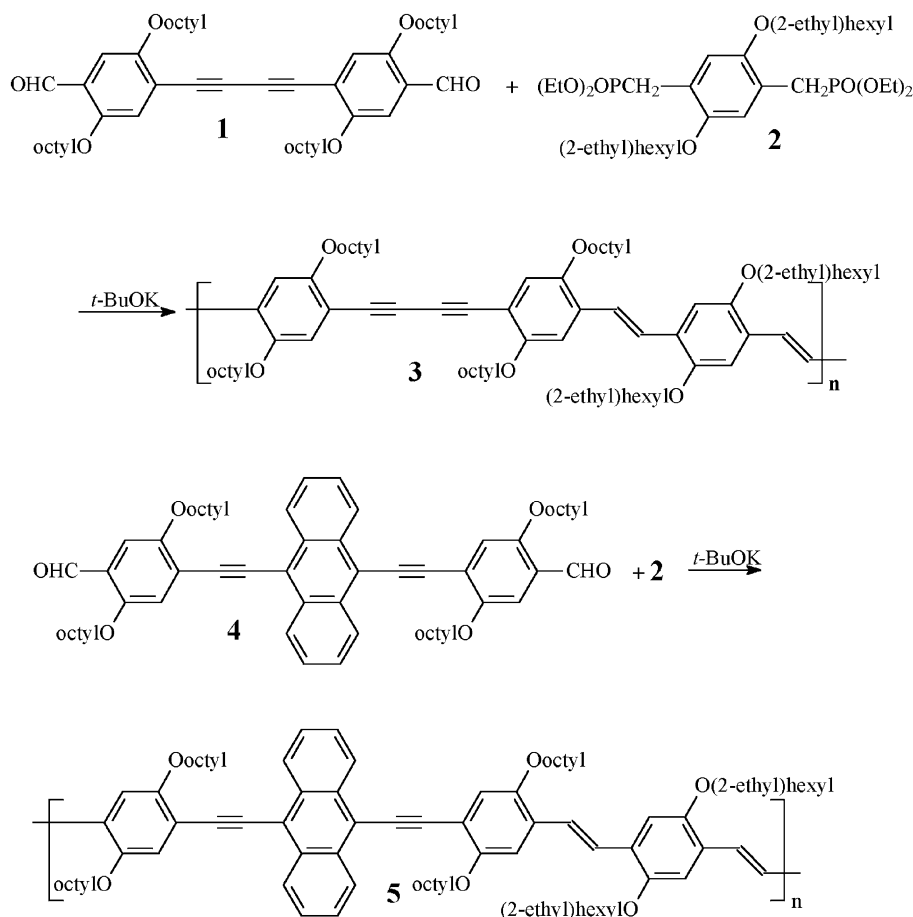


Fig. 2 Schematic structure of the plastic solar cells. The active layer consists of a blend of a conjugated polymer and the fullerene PCBM and has a thickness around 50 to 100 nm. The PEDOT : PSS layer spin cast from aqueous solution is about 80 nm thick.



Scheme 1 Synthetic path to the polymers 3 and 5.

electrodes were platinum foils. The reference electrode (RE) was a silver wire coated with AgCl.

In the EVS method the electrode potential was varied in 10 mV steps covering a range of 400 mV around the expected onset of oxidation and reduction, respectively. After each step the potential was kept constant for 1 minute to attain quasi-equilibrium conditions. If oxidation or reduction takes place, an abrupt increase of the current is observed. While the potential is kept constant, this current decays to the baseline until no more charges can be injected into the polymer at that certain potential. Integration of these data over time gives the change of the injected charges with the potential $\Delta Q/\Delta E$, which can be plotted vs. E and can be interpreted as an infinitesimally slow cyclic voltammogram.

The morphology of the active layers was investigated by tapping mode AFM measurements, using a Dimension 3100 system (Digital Instruments, Santa Barbara, CA).

3. Results and discussion

Scheme 1 shows the synthetic path to the polymers 3 and 5. They were synthesized through the Horner–Wadsworth–Emmons olefination reactions of fluorophoric dialdehydes 1 [1,4-bis(4-formyl-2,5-dioctyloxyphenyl)butadiyne-1,3]²³ and 4 {9,10-bis[(4-formyl-2,5-dioctyloxy)phenylethynyl]anthracene}²⁴ with 2,5-di(2'-ethyl)hexyloxy-*p*-xylylene-bis(diethylphosphonate) (2).²⁵ Polymer 3 was obtained as a orange red material in 80% yield.²³ The anthracene-containing polymer 5 was obtained as a dark red material in 77% yield. The molecular weights were estimated through gel-permeation chromatography with polystyrene as standard while using tetrahydrofuran as eluent. Polymer 3 has a \bar{M}_n value of 24 000 g mol⁻¹ and a \bar{M}_w value of 70 000 g mol⁻¹ leading to a polydispersity index (PDI) of 2.9 and a degree of polymerization (DP) of 22. Polymer 5 has following

characteristics: $\bar{M}_n = 11\,000$ g mol⁻¹, $\bar{M}_w = 36\,000$ g mol⁻¹, PDI = 3.0. and DP = 9. The chemical structures of the compounds were confirmed through ¹H NMR, ¹³C NMR, elemental analysis and infrared (IR) spectroscopy. They are thermostable up to around 330–350 °C, where approximately 5% weight loss was observed.

The absorption and emission behaviors of both compounds were investigated in dilute chloroform solution as well as in thin films, obtained after spin casting from chlorobenzene solutions on a thin glass substrate. The absorption maxima, λ_a , the absorption coefficients at the maximum of the absorption, ϵ_{\max} , the emission maxima, λ_e , the optical band gap energies, E_g^{opt} , and the fluorescence quantum yields, ϕ_f , are given in Table 1. The emission spectra were obtained after exciting at the wavelength of the absorption maximum. The solution and solid-state absorption and emission spectra of 3 and 5 are shown in Figs. 3 and 4 respectively. Polymer 3 absorbs in solution at $\lambda_a = 484$ nm ($E_g^{\text{opt}} = 2.34$ eV) and emits at $\lambda_e = 528$ nm leading to a Stokes shift of 44 nm. Its solution emission spectrum consists moreover of a shoulder around 569 nm; a very high fluorescence quantum yield of 85% was obtained. The

Table 1 Data from UV-Vis absorption and photoluminescence investigations in dilute chloroform solution and in thin films

Compound	λ_a/nm	$\epsilon_{\max}/\text{M}^{-1} \text{cm}^{-1}$	E_g^{optd}	λ_e/nm	ϕ_f (%) ^c
3 ^a	484	91 000	2.34	528 (sh: 569)	85
3 ^b	498, 520	—	2.20	552, 592	23
5 ^a	540	77 300	2.12	580	53
5 ^b	552, 575	—	1.90	620 (sh: ~670)	12

^a Solution. ^b Thin film. ^c Per mole of the repeating unit. ^d $E_g^{\text{opt}} = hc/\lambda_{10\% \text{ max}}$, with $\lambda_{10\% \text{ max}}$ considered as 10% of the absorption maximum (taken from the lower energy side of the spectrum).²³ ^e Fluorescence quantum yield $\pm 10\%$.

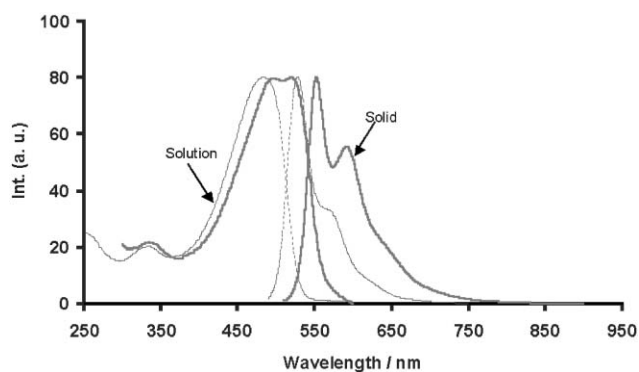


Fig. 3 Solution (---) and solid state (—) absorption and emission spectra of polymer 3.

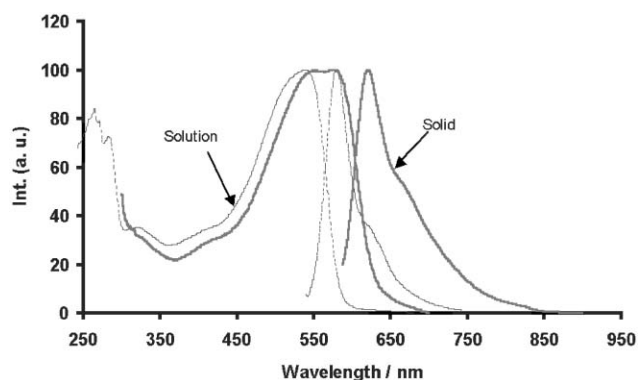


Fig. 4 Solution (---) and solid state (—) absorption and emission of polymer 5.

solid-state absorption and emission spectra of **3** are red shifted relative to the solution due to enhanced planarisation and aggregate formation. The solid-state absorption spectrum consists of a broad peak having two maxima at $\lambda_a = 498$ nm and 520 nm ($E_g^{opt} = 2.20$ eV). The well-structured solid-state emission spectrum of **3** is made up of two peaks centered at $\lambda_e = 552$ nm and 592 nm respectively leading to a Stokes shift of 32 nm. A fluorescence quantum yield of 23% was obtained.

The presence of the electron rich anthracene is at the source of the bathochromic shift of polymer **5** relative to **3**. The solution absorption spectrum of **5** has its maximum at $\lambda_a = 540$ nm ($E_g^{opt} = 2.12$ eV); its emission spectrum is centered at $\lambda_e = 580$ nm, leading to a Stokes shift of 40 nm and a fluorescence quantum yield of 53%. Similar to the case of **3**, the broad solid-state absorption peak of **5** is made up of two maxima at $\lambda_a = 552$ nm and $\lambda_a = 575$ nm ($E_g^{opt} = 1.90$ eV). A narrow solid-state emission curve was obtained for **5**. It consists of a maximum at $\lambda_e = 620$ nm and a weak shoulder around 670 nm. A fluorescence quantum yield of 12% was obtained.

For the evaluation of the molecular energy levels, cyclic voltammetry (CV) and electrochemical voltage spectroscopy (EVS) measurements were applied (Fig. 5). From the graph it can easily be seen that there are strong variations in the HOMO and LUMO levels of the several polymers applied. On going from MDMO-PPV over polymer **5** to polymer **3**, the HOMO level is lowered by 250 mV, while the LUMO levels vary in the same manner by 310 mV. The electrochemical band-gaps are equal for MDMO-PPV and polymer **3**, but that of polymer **5** is lower. The electrochemical results are summarized in Table 2.

In Fig. 6 the photocurrent spectra of some typical devices are shown. From these measurements it appears that the optical band-gap of polymer **3** is in fact larger than that of MDMO-PPV, while polymer **5** has a far broader absorption range extending up to 630 nm. The external quantum efficiencies for

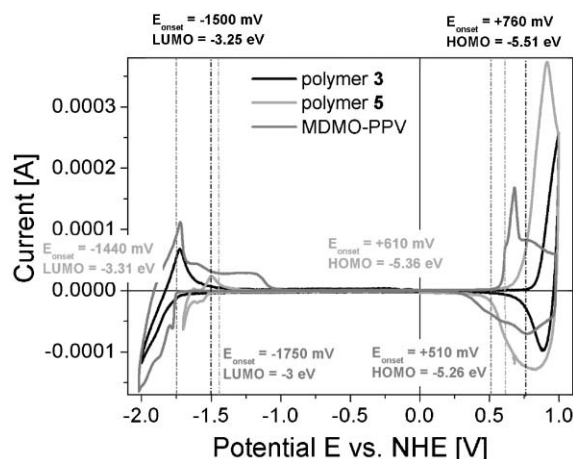


Fig. 5 Cyclic voltammograms of polymer **3**, polymer **5** and MDMO-PPV; onset potentials determined with EVS are indicated through broken lines.

Table 2 Molecular energy levels as determined by electrochemical voltage spectroscopy

Compound	HOMO/eV	LUMO/eV	E_g /eV
3	-3.25	-5.51	2.26
5	-3.31	-5.36	2.05
MDMO-PPV	-3	-5.26	2.26

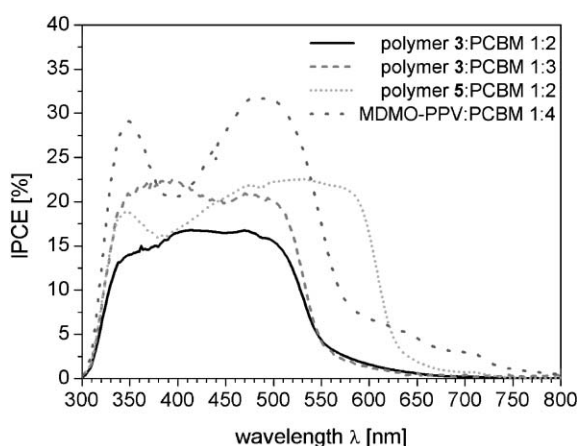


Fig. 6 Spectral photocurrent of different devices studied. The larger photocurrent for polymer **3** : PCBM 1 : 3 as compared to 1 : 2 may follow from improved percolation and a smaller film thickness and thus charge transport. However, the external quantum efficiencies of polymers **3** and **5** are generally below that of MDMO-PPV.

polymer **3** and polymer **5** exceed only slightly 20%. This was a main limiting factor for the short circuit current I_{SC} (compare with Fig. 7) of the investigated devices. The short circuit current of the polymer **3** based device stayed far below that of the MDMO-PPV : PCBM device, while the devices based on polymer **5** were comparable. This can be understood, since the broader absorption of polymer **5** will directly result in an increased photocurrent, even at the low external quantum efficiencies obtained. Interestingly the maximum open circuit voltages V_{OC} followed the trend in the HOMO levels of the polymers found with the EVS measurements. For the PEDOT : PSS (Baytron PH) used here as anode, blends with different PCBM contents ranging between 66% and 80% yielded with MDMO-PPV 800 to 840 mV, polymer **5** gave 820 to 850 mV and polymer **3** resulted in 850 to 900 mV. Thus this study supports the idea about the origin of the open circuit potential being the quasi-Fermi level splitting between the donor HOMO and the acceptor LUMO. Hence the lowering of the HOMO

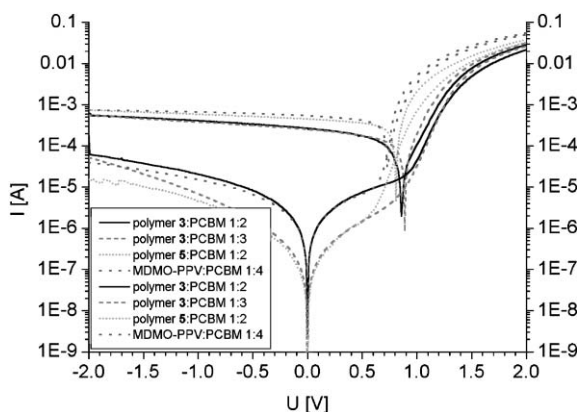


Fig. 7 Current-voltage characteristics of the investigated devices, measured in the dark (lower left, with $I = 0$ A at $U = 0$ V) and under 80 mW cm^{-2} AM 1.5 solar simulator illumination (upper right).

levels can be an important factor for improved device efficiencies. The lower HOMO level or ionization potential of the PPV-PPE polymers results from the triple bonds (PPE groups) inside the polymer backbone, thus this class of

materials may provide a route towards increased open circuit voltages in polymer/fullerene based photovoltaic devices. The highest power conversion efficiency of 2% for the PPV-PPE : PCBM blends studied was achieved with polymer 5 : PCBM (1 : 2) under 100 mW cm^{-2} AM 1.5 solar simulator illumination. The device yielded a photocurrent of about 4.3 mA cm^{-2} , an open circuit voltage of 810 mV and a filling factor of 59%.

Using AFM measurements, the origin of the relatively small external quantum efficiencies and thus photocurrents could be attributed to a large scale phase separation in the PPV-PPE : PCBM blends (compare Fig. 8). The domain sizes in the phase separation are of the order of 100–200 nm, comparable to the MDMO-PPV : PCBM devices spin cast from toluene.^{6,7} Hence it is expected that some of the photoexcitations will not lead to separate charge carriers and may recombine within the large clusters.

Comparison of the topography of polymer 3 : PCBM 1 : 2 (by weight) (Fig. 8b) with polymer 3 : PCBM 1 : 3 (Fig. 8c) shows that the larger PCBM concentration in the casting solution will lead to the larger scale of phase separation. This is in agreement with ratio studies for the MDMO-PPV : PCBM system,^{6,7} where an increasing PCBM content led similarly to larger clusters in the spin cast films. While the MDMO-PPV :

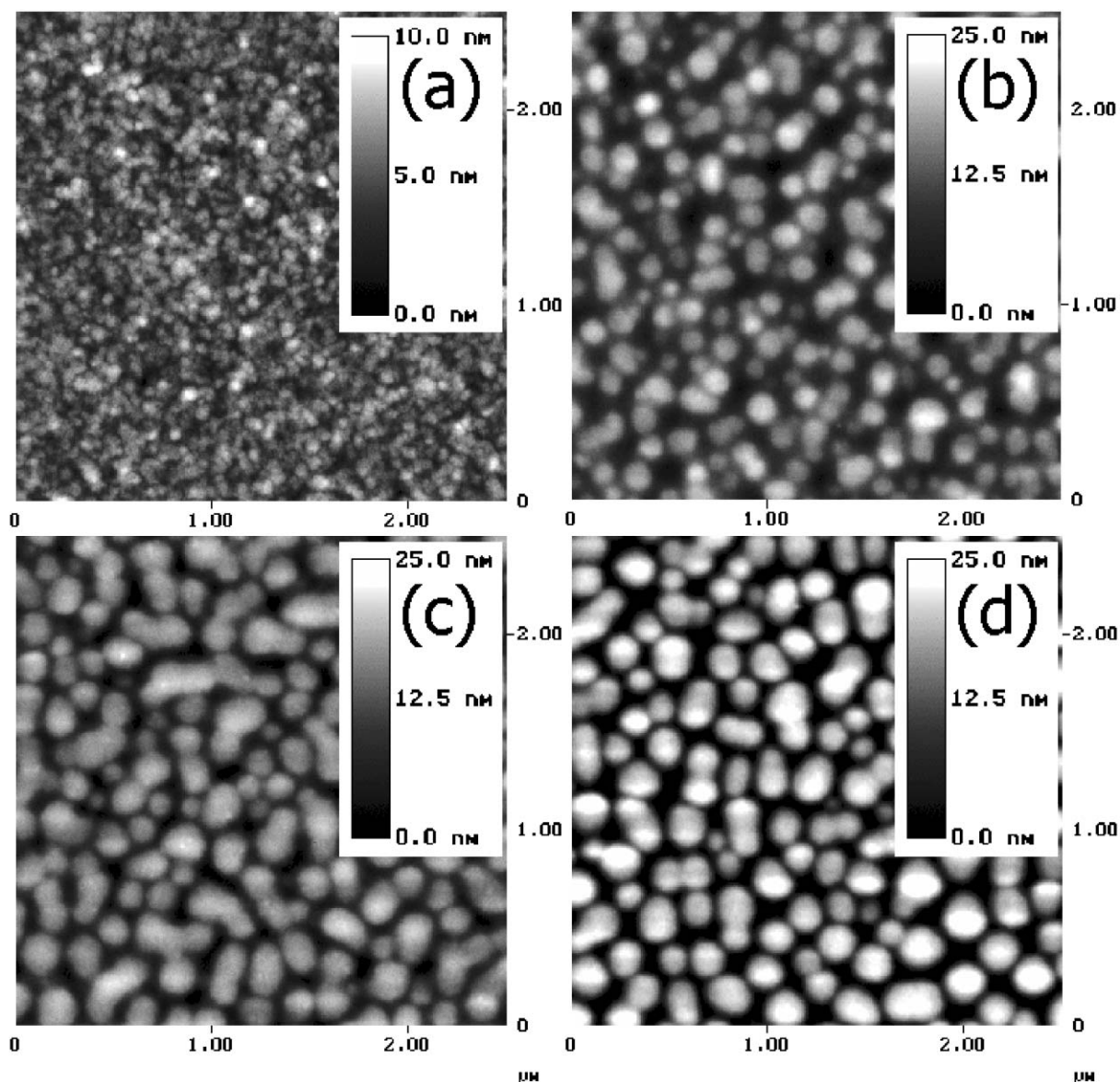


Fig. 8 Tapping mode scanning probe microscopy on the active layers of the devices under investigation here. In (a) the topography of the MDMO-PPV : PCBM 1 : 4 blend film is depicted. (b), (c) and (d) show the polymer 3 : PCBM 1 : 2, polymer 3 : PCBM 1 : 3 and polymer 5 : PCBM 1 : 2 blend films respectively. For a larger PCBM content, larger clusters are observed (b, c).

PCBM cast film shows a rather smooth surface, a coarse grained nanomorphology in the films consisting of PPE-PPV donors in blend with PCBM seems to be the main limiting factor of the photocurrent generation.

4. Conclusion

Polymer/fullerene bulk heterojunction solar cells were prepared successfully from novel PPV-PPE hybrid copolymers with PCBM. Due to the lower HOMO levels of these polymers in comparison to MDMO-PPV, larger open circuit voltages could be obtained. Due to a coarse nanoscale morphology within these blends the photocurrent was smaller than for a comparable MDMO-PPV based device. Further work will be dedicated to optimizing the morphology of these blends.

Acknowledgements

Financial support was provided by the German Ministry for Education and Research (BMBF, contract number 01SF0119). Part of this work was performed within the Christian Doppler Society's dedicated laboratory on Plastic Solar Cells.

References

- 1 C. J. Brabec, N. S. Sariciftci and J. C. Hummelen, *Adv. Funct. Mater.*, 2001, **11**, 15.
- 2 J. Nelson, *Curr. Opin. Solid State Mater. Sci.*, 2002, **6**, 87.
- 3 *Organic Photovoltaics: Concepts and Realization*, vol. 60, ed. C.J. Brabec, V. Dyakonov, J. Parisi, and N.S. Sariciftci, Springer, Berlin, 2003.
- 4 N. S. Sariciftci, L. Smilowitz, A. J. Heeger and F. Wudl, *Science*, 1992, **258**, 1474.
- 5 S. E. Shaheen, C. J. Brabec, N. S. Sariciftci, F. Padinger, T. Fromherz and J. C. Hummelen, *Appl. Phys. Lett.*, 2001, **78**, 841.
- 6 T. Martens, J. D'Haen, T. Munters, Z. Beelen, L. Goris, J. Manca, M. D'Olieslaeger, D. Vanderzande, L. D. Schepper and R. Andriessen, *Synth. Met.*, 2003, **138**, 243.
- 7 H. Hoppe, M. Niggemann, C. Winder, J. Kraut, R. Hiesgen, A. Hinsch, D. Meissner and N. S. Sariciftci, *Adv. Funct. Mater.*, 2004, **14**, in print.
- 8 F. Padinger, R. S. Rittberger and N. S. Sariciftci, *Adv. Funct. Mater.*, 2003, **13**, 1.
- 9 A. Dhanabalan, J. K. J. van Duren, P. A. van Hal, J. L. J. van Dongen and R. A. J. Janssen, *Adv. Funct. Mater.*, 2001, **11**, 255.
- 10 K. Colladet, M. Nicolas, L. Goris, L. Lutsen and D. Vanderzande, *Thin Solid Films*, 2004, **451-452**, 7.
- 11 C. Winder and N. S. Sariciftci, *J. Mater. Chem.*, 2004, **14**, 1077.
- 12 M. M. Wienk, J. M. Kroon, W. J. H. Verhees, J. Knol, J. C. Hummelen, P. A. v. Hall and R. A. J. Janssen, *Angew. Chem., Int. Ed.*, 2003, **42**, 3371.
- 13 C. J. Brabec, A. Cravino, D. Meissner, N. S. Sariciftci, T. Fromherz, M. T. Rispens, L. Sanchez and J. C. Hummelen, *Adv. Funct. Mater.*, 2001, **11**, 374.
- 14 H. Kim, S.-H. Jin, H. Suh and K. Lee, Origin of the open circuit voltage in conjugated polymer-fullerene photovoltaic cells, in *Organic Photovoltaics IV*, ed. Z.H. Kafafi, and P.A. Lane, Proceedings of SPIE, Int. Soc. Opt. Eng., Bellingham, WA, USA, 2004, Vol. 5215, p. 111.
- 15 A. Gadisa, M. Svensson, M. R. Andersson and O. Inganäs, *Appl. Phys. Lett.*, 2004, **84**, 1609.
- 16 H. Frohne, S. E. Shaheen, C. J. Brabec, D. C. Müller, N. S. Sariciftci and K. Meerholz, *ChemPhysChem*, 2002, **9**, 795.
- 17 V. D. Mihailetschi, P. W. M. Blom, J. C. Hummelen and M. T. Rispens, *J. Appl. Phys.*, 2003, **94**, 6849.
- 18 G. Brizius, N. G. Pschirer, W. Steffen, K. Stitzer, H. C. zur Loye and U. H. F. Bunz, *J. Am. Chem. Soc.*, 2000, **122**, 12435.
- 19 A. M. Ramos, M. T. Rispens, J. K. J. van Duren, J. C. Hummelen and R. A. J. Janssen, *J. Am. Chem. Soc.*, 2001, **123**, 6714.
- 20 A. P. H. Schenning, A. C. Tshipis, S. C. J. Meskers, D. Beljonne, E. W. Meijer and J. L. Brédas, *Chem. Mater.*, 2002, 14.
- 21 Q. Chu, Y. Pang, L. Ding and F. E. Karasz, *Macromolecules*, 2003, **36**, 3848.
- 22 T. Yamamoto, W. Yamada, M. Takagi, K. Kizu, T. Maruyama, N. Ooba, S. Tomaru, T. Kurihara, T. Kaino and K. Kubota, *Macromolecules*, 1994, **27**, 6620.
- 23 D. A. M. Egbe, C. Bader, J. Nowotny and E. Klemm, Synthesis and characterization of three types of alkoxy-substituted hybrid PPV-PPE polymers: Potential candidates for photovoltaic applications, in *Organic Photovoltaics IV*, ed. Z.H. Kafafi, and P.A. Lane, Proceedings of SPIE, Int. Soc. Opt. Eng., Bellingham, WA, USA, 2004, vol. 5215, p. 79.
- 24 D. A. M. Egbe, C. Bader, J. Nowotny, W. Günther and E. Klemm, *Macromolecules*, 2003, **36**, 5459.
- 25 D. A. M. Egbe, C. P. Roll, E. Birckner, U.-W. Grummt, R. Stockmann and E. Klemm, *Macromolecules*, 2002, **35**, 3825.
- 26 J. N. Demas and G. A. Crosby, *J. Phys. Chem.*, 1971, **75**, 991.